sciendo

POLISH MARITIME RESEARCH Special Issue 2018 S3 (99) 2018 Vol. 25; pp. 68-77
10.2478/pomr-2018-0114

NUMERICAL SIMULATIONS OF LINEARLY STRATIFIED FLOW PAST SUBMERGED BODIES

Weizhuang Ma[1]
Yunbo Li[2]
Yong Ding[1]
Kaiye Hu[1]
Linxin Lan[1]
[1] College of Shipbuilding Engineering, Harbin Engineering University, China
[2] College of Ocean Science and Engineering, Shanghai Maritime University, China

ABSTRACT

In this study, a methodology was presented to predict density stratified flows in the near-field of submerged bodies. The energy equation in temperature form was solved coupled with momentum and mass conservation equations. Linear stratification was achieved by the definition of the density as a function of temperature. At first, verifications were performed for the stratified flows passing a submerged horizontal circular cylinder, showing excellent agreement with available experimental data. The ability of the method to cope with variable density was demonstrated. Different turbulence models were used for different Re numbers and flow states. Based on the numerical methods proposed in this paper, the stratified flow was studied for the real scale benchmark DAPRA Suboff submarine. The approach used the VOF method for tracing the free surface. Turbulence was implemented with a k – ω based Detached Eddy Simulation (DES) approach. The effects of submarine speed, depth and density gradient on the free surface wave pattern were quantitatively analyzed. It was shown that, with the increasing of the speed of the submarine, the wavelength and wave height of the free surface wave were gradually increasing. The wave height of the free surface wave was gradually reduced as the submarine's depth increased. Relative to the speed and submarine depth, the changes of the gradient density gradient have negligible effects on the free surface wave field.

Keywords: Stratified flow, circular cylinder, internal wave, Suboff, equation of state

INTRODUCTION

As is known to us all, the ocean is density stratified especially in the vertical direction. When a submerged body moves in the ocean, it can leaves a lot of wake features because of the stratification effect. It also can produce some singular flow phenomena which are different from those in the uniform flow environment. For instance, lee waves can be observed clearly in the wake of the submerged bodies when they are moving at low speeds. These characteristic wakes will cause some changes in the wind waves on the free surface. For example, the wave amplitude on the free surface may be converged and diverged for a long time [1-3]. Beside, a lot of researchers describe the formation of lee waves for the flows around cylinders with different Froude number(*Fr*) based on the methods of asymptotic analysis [4-6]. Many other researchers also study the linearized density stratified flow passing a circular cylinder by experimental methods [7-10]. Meunier showed experimentally and numerically that vortices can be emitted for strong stratifications at moderate Reynolds numbers [11].

There are fewer numerical works on the flow around a cylinder in a linear stratified fluid. Meunier described numerically how the three-dimensional instabilities of a cylinder wake are modified by the presence of a linear density stratification [12]. Boyer has founded a large number of regimes when the *Fr* varies from 0.02 to 13 and the Reynolds number (*Re*) varies from 5 to 4000. For the condition of being

strongly stratified, the study revealed the presence of internal waves, of an accelerated flow on the centerline. Winters and Armi studied the recirculation bubble upstream of the cylinder, which is known as the blocking effect [13]. The stratification seemed to prevent the appearance of vortices, due to the stabilization of the stratification. Stratified wakes of other real scaled submerged body have received less attention. Esmaeilpour has studied the stratified flow around naval vessels. It is shown that the generation of internal waves requires energy that results in an increase in resistance [14]. Chang presented the CFD computations for a vessel in a stratified fluid. They computed the internal and surface waves generated by the DARPA Suboff submarine advancing in a two-layer fluid, for different Froude numbers, and studied the wave pattern [15].

In this paper, the continuity equation and the momentum conservation equation were solved for the motion of the flow. The energy equation was used to introduce the temperature into the numerical method. The equations were closed by the 1980 international standard seawater equation of state in order to realize the density stratification of the fluid. Numerical simulations of stratified flow passing a cylinder were conducted in order to verify the validity of the methods. The simulations cover from low *Fr* number to the high *Fr* number. The numerical results agree well with the experimental results of Boyer. Then, the established method was used to analyze the stratified flow past the real-scale Suboff submarine flow. The influences of speed, depth and stratification characteristics on the free surface wave of the submarine are analyzed.

NUMERICAL METHEOD

GOVERNING EQUATIONS

Since the speed of the submerged body is comparatively very low, the flow is still in the category of incompressible fluid. The continuity equation and the momentum conservation equation can be used to solve the fluid motion. The energy conservation equation in terms of temperature is used to introduce the density anomaly into the numerical method. Finally, the 1980 standard seawater equation of state is used to realize the closure of the equations. The basic governing equations for numerical solution are expressed as follows.

$$\frac{\partial \rho}{\partial t} + \nabla \cdot (\rho \vec{v}) = 0 \tag{1}$$

$$\frac{\partial}{\partial t}(\rho \vec{v}) + \nabla \cdot (\rho \vec{v}\vec{v}) = -\nabla p + \nabla \cdot (\bar{\bar{\tau}}) + \rho \vec{g} \tag{2}$$

$$\frac{\partial (\rho T)}{\partial t} = -\nabla \cdot (\rho \vec{u} T) + \nabla \cdot (\frac{k}{c} \nabla (T)) \tag{3}$$

In the above formula, T is the temperature, and the unit is K. According to the 1980 standard seawater state equation, the water density can be expressed as a function of temperature and salinity. This study only discusses the effect of temperature on density. In the calculation process, only the linear part of the temperature in the equation of state was taken into account. The detailed functional relationship between temperature and density is:

$$\rho(T, S) = \rho_0 + AS + BS^{3/2} + CS \tag{4}$$

$$A = 8.24493 \times 10^{-1} - 4.0899 \times 10^{-3} (T - 273.15) \tag{5}$$

$$B = -5.72466 \times 10^{-3} + 1.0227 \times 10^{-4} (T - 273.15) \tag{6}$$

$$C = 4.8314 \times 10^{-4} \tag{7}$$

$$\rho_0 = 999.842594 + 6.793952 \times 10^{-2} (T - 273.15) \tag{8}$$

In order to verify the accuracy of the numerical method in this paper, the flow characteristics around the cylinder in the stratified flow are first analyzed. The computational domain diagram and mesh of this study is shown on Figure 1. Some dimensionless parameters used in this paper are:

Internal Froude number,

$$Fr = \frac{U}{ND} \tag{9}$$

Reynolds number,

$$Re = \frac{UD}{\upsilon} \tag{10}$$

Dimensionless time,

$$t_n' = \frac{t_n U}{d} \tag{11}$$

$$t_e' = \frac{t_e U}{d} \tag{12}$$

Where is the flow velocity, and d is the diameter of the cylinder, t_n is the flow time in numerical simulation and t_e is the flow time in the experimental conditions, t_n' is the dimensionless time for numerical simulations, t_e' is the

dimensionless time for the experiments, υ is the kinematics viscosity coefficient of water, N is the buoyancy frequency:

$$N = \sqrt{-\frac{g}{\rho_0}\frac{\Delta\rho}{H}} \tag{13}$$

g is the acceleration of gravity, and other parameters for N are shown in Figure 1(a).

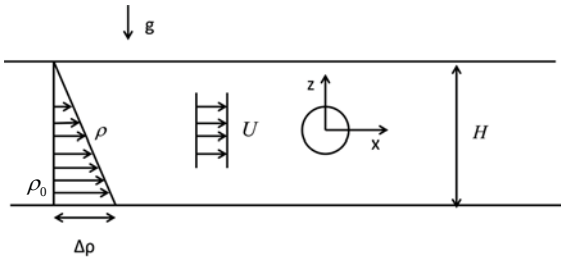

(a) Computational domain diagram

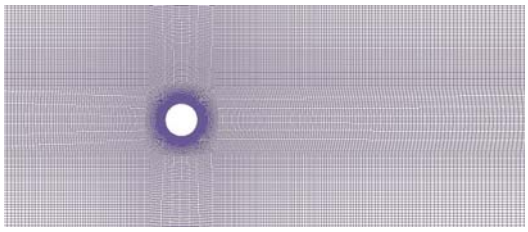

(b) Mesh around the cylinder

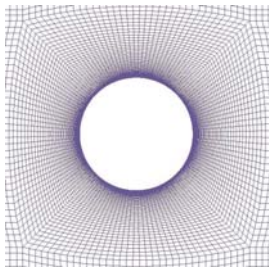

(c) O-block around the cylinder

Fig.1. Computational domain

Through the above process, the density of the fluids is linearly stratified. In order to be consistent with the experimental conditions of Boyer, the height of the fluid field is 0.2m, the cylinder diameter is 0.024m, and the inlet and outlet boundaries are far enough. The reference density is $\rho_0 = 998$ kg/m^3, and density change is $\Delta\rho = 20.58$ kg/m^3, then the buoyancy frequency is $N = 1.0$ (1/s).

According to the theory research of Boyer, when the Fr number is small, there are lee waves in the wake, and when the Fr number is large, the vortex structure in the wake plays a key role. Through the test of Boyer, when the Fr reaches to 0.4, the main features in the wake are already not the lee wave, and then the vortex structure in the wake is getting the upper hand. According to this conclusion, we define the Fr >0.4 is high, and the Fr <0.4 number is low.

The main operating conditions and specific settings are shown in Table 1. The numerical results are compared with the experimental results of Boyer.

Tab. 1. Conditions of stratified flow around a cylinder

Index		*Fr*	*Re*
1	Low *Fr*	0.018	12
2		0.08	1500
3	High *Fr*	0.88	480
4		1.77	960

NUMERICAL RESULTS OF THE STRATIFIED FLOW AROUND THE CYLINDER

THE NUMERICAL RESULTS FOR LOW *FR*

In this paper, the numerical simulation of the stratified flow around a circular cylinder at low *Fr* is performed. The streamline pattern of the numerical simulation and the experimental results are shown in Figure 2.

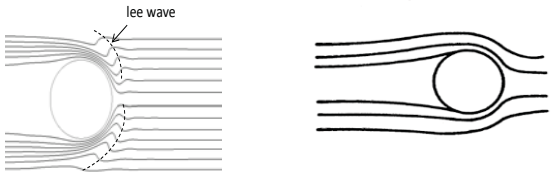

(a) numerical result (b) experimental result of Boyer

Fig.2. Streamline for Fr=0.018, Re=12

It can be seen that the numerical results are consistent well with the experimental results. There are also some differences in the numerical results, and the lee wave wake pattern of the cylinder is symmetric due to the volume effect of the cylinder. Also, the lee wave peak line is asymmetric up and down. There is no new lee wave generation in the direction of flow. Figure 3 shows the velocity profile of the numerical results at $x = \pm 7.5d$ when t_n' =11, 22 and 54. Figure 3(a) is the velocity profile curve for the upstream and Figure 3(b) is the velocity profile curve for the downstream. The flow diagram shows that the velocity crest value of upstream velocity profile and the velocity trough value of the downstream velocity profile are all increasing with time. The flow formed in the stratified flow is a quasi steady state, and the velocity profile is slightly different at different time.

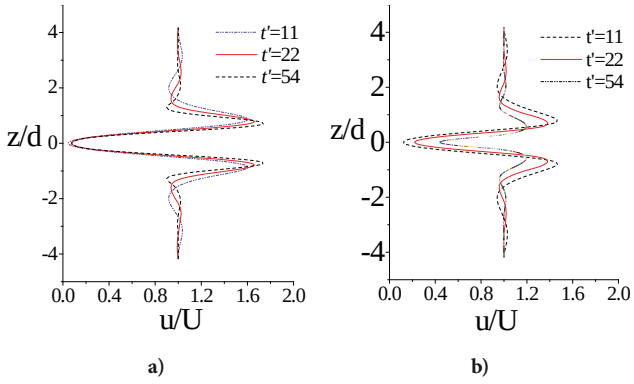

Fig. 3. Numerical results of velocity profiles upstream and downstream of cylinder at $x = \pm 7.5d$ for Fr=0.018, Re=12, $t_n' = 11,22,54$.

Figure 4 is the velocity profile curve at $t_e' = 21$, 42 and 62, in which Figure 4(a) is the velocity profile curve for the upstream and Figure 4(b) is the velocity profile curve for the downstream. The study shows that the downstream speed profile curve is "two sections curve" with the relative speed less than 1.0 in the near of the axis. The velocity profile of the numerical results is qualitatively consistent with the experimental results.

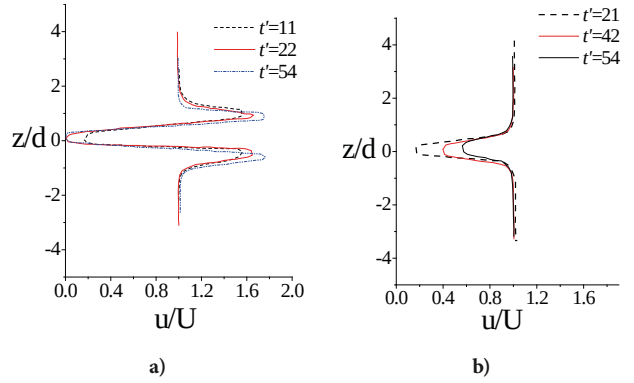

Fig. 4. Experimental results of velocity profiles upstream and downstream of cylinder at for Fr=0.018, Re=12, $t_e' = 21,42,62$

The numerical time is not corresponding to the experimental time in the beginning. However, in a numerical moment, if the upstream velocity profile is corresponding to the test time, then the downstream velocity profile of the numerical results will bring into correspondence with the test results at the same time during the subsequence. Figure 5 shows the numerical results of $x = \pm 7.5d$ at $t_n' = 15$ and $t_n' = 67$. The comparison of the numerical results to the experimental velocity profile at $t_e' = 21$ and $t_e' = 62$ can verify this rule. The extreme of the velocity profile represents the maximum or minimum value of the velocity somewhere. The relative error of the trough is less than 2%. This proves that the numerical results agree well with experimental results quantitatively. This proposed model is an effective method for the simulation of the internal wake at low *Fr* number.

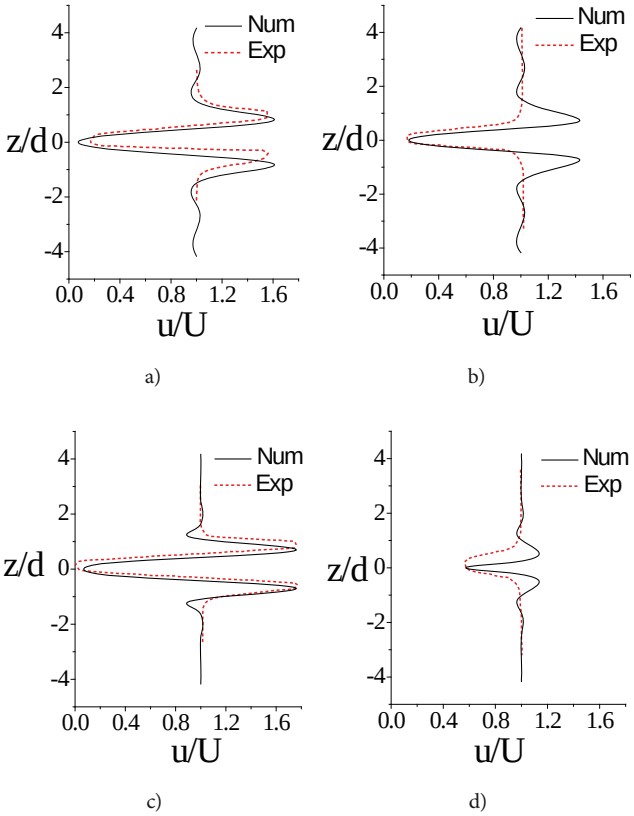

Fig. 5. Velocity profiles upstream and downstream of cylinder under numerical and experimental conditions. (a, c) upstream; (b, d) downstream

THE INFLUENCE OF TURBULENCE MODEL ON NUMERICAL RESULTS

Based on the previous work for low *Fr*, keeping the same *Fr* =0.08, we change the speed and the characteristic length of the cylinder in order to get different numerical simulation results for Reynolds number varying from 240 to 6000. It was found that the wake characteristics are similar below the *Re* =98.7. It shows that the flow line is "calabash shape" near the axis and also the lee wave is generated behind the cylinder. The results for different turbulence models at *Re* =1500 are shown in Figure 6.

We can find that the characteristics of the wake and the "calabash shape" streamline feature in the wake of the RSM model results are the closest to that in the laminar flow model. The SST $k-\omega$ model is more similar to the laminar state [17]. The $k-\varepsilon$ model results are relatively largely different with the laminar model. For the lee wave characteristics in the wake, the results under RSM model are in good agreement with the laminar model results. There is only one pair of lee wave in the results of $k-\varepsilon$ model. The lee wave of the SST $k-\omega$ model decays very quickly, and there are only two pairs of lee waves. In fact, the turbulence model is based on the assumption of the eddy viscosity hypothesis and isotropic [18]. But in the density stratified fluids, the density is not isotropic, so it is more reasonable to use the RSM model which is not restricted by isotropy assumption. It is worth

mentioning that in the implementation of the RSM model, we use the wall function to deal with the near wall. If it uses the enhanced wall function and the result is similar to that of the SST $k-\omega$ model under the same condition. When it comes to the $k-\varepsilon$ model, there is no difference between the results of the SST $k-\omega$ model using the wall function and the enhanced wall function. It has the same conclusion between the Re=6000 and the Re=1500 [19].

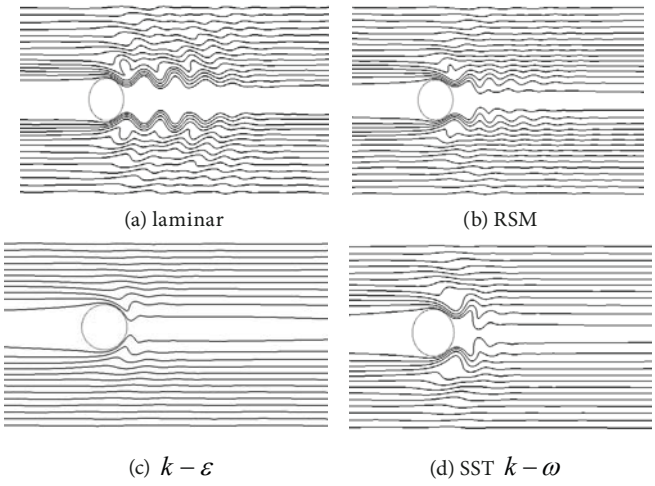

(a) laminar (b) RSM

(c) $k-\varepsilon$ (d) SST $k-\omega$

Fig. 6. The numerical results under different turbenlence models

THE NUMERICAL RESULTS FOR HIGH *FR*

This paper uses the $k-\omega$ based DES model to study the wake of the cylinder at high *Fr* in the stratified flows. Figure 7 shows the experimental results and numerical results of the flow around a circular cylinder under the condition of *Fr*=0.88 and *Re*=480. The two results are roughly the same for the wake streamline shape. Also, they both have a pair of vortices in the wake behind the cylinder [20]. The first wave packet generates at a distance of 6 times than the diameter of the cylinder center. The second wave packets generates at a distance of 16 times than the diameter of the cylinder center. The difference is that wave package amplitude of numerical results is smaller than the experimental results. In fact, in order to keep consistent with experiment, the distance from the center of the cylinder to the upper and lower bound is 4.17*d*. Thus, there is a non-negligible effect for the boundary conditions during the numerical simulations [21]. Also, the experiment takes the manner of dragging a cylinder, so the boundary conditions of the physical tank are relatively small. Figure 8 shows the experimental results and numerical results of the flow around a circular cylinder under the condition of *Fr*=1.77and *Re*=960. The typical characteristics of the wake in this condition are that the wake presents fully turbulent wake state. There is a strong vortex structure near the cylinder wake. Obviously, the numerical method successfully simulates these features.

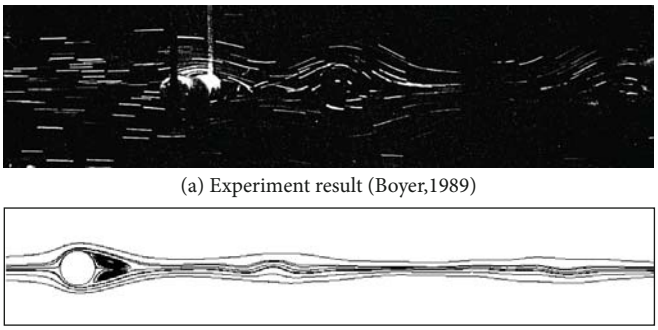

(a) Experiment result (Boyer,1989)

(b) Numerical result

Fig.7. Experimental and numerical results for Fr = 0.88, Re = 480

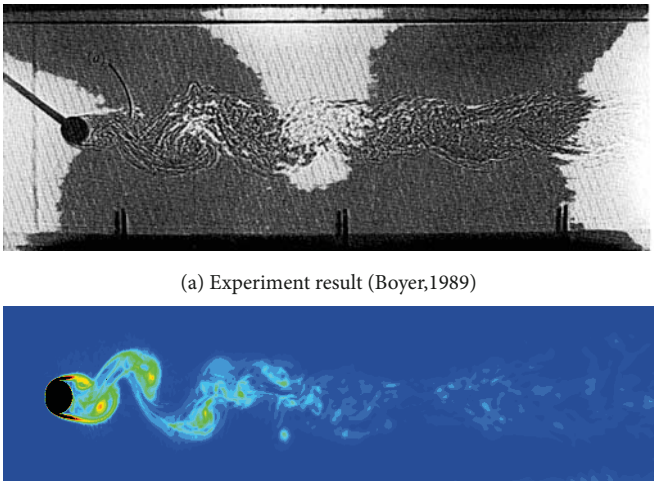

(a) Experiment result (Boyer,1989)

(b) Numerical result

Fig. 8. Experimental and numerical results for Fr = 1.77, Re = 960

NUMERICAL RESULTS OF THE STRATIFIED FLOW AROUND SUBOFF

Based on the numerical method established above, the numerical simulations of the flow field of the moving submarine in the mixed stratified flow are carried out. The simulated submarine uses the well-known DARPA Suboff full-appended model, and the model is magnified 20 times to obtain a real-scale submarine. The main particulars of the Suboff model and the simulated real scale model are shown in Table 2.

Tab. 2. Main particulars of the Suboff model

	Suboff Model	Simulation Model
L_{OA} (m)	4.356	87.12
L_{BP}	4.261	85.22
D_{max}	0.508	10.16
S (m^2)	5.989	2395.6
∇ (m^3)	0.699	5592

In order to accurately capture the flow field details and flow in the turbulent state, this paper uses the turbulence model of $k-\omega$ based detached eddy simulation (DES) method to numerically simulate the stratified flow around the Suboff submarine. The convective item discrete format adopts the bounded center difference format. The diffusion item discrete format uses a central difference format, and the time item discrete format uses a second order up wind format [22]. At the same time, because the flow around the Suboff is a transient problem, the discrete equation is solved by PISO algorithm. The computational geometry models related to this paper have a variety of absolute dimensions. Each calculation case uses three sets of grids to perform the correlation verification process on grid independence, confirming the convergence of the grid. The geometric model and the 3-D view of the Suboff model with full appendages is shown in Figure 9.

Fig. 9. The 3-D view of the Suboff model

Since the calculations are implemented on the real scale submarine, the calculation domain needs to be large enough in order to fully capturing the hydrodynamic phenomenon in the wake field. Figure 10 is a schematic diagram of the calculation domain. The extension of the incoming flow direction is 200m, and the distance of the wake direction behind the Suboff is 1000m. The calculation domain lengths of the right and left side are 500m.

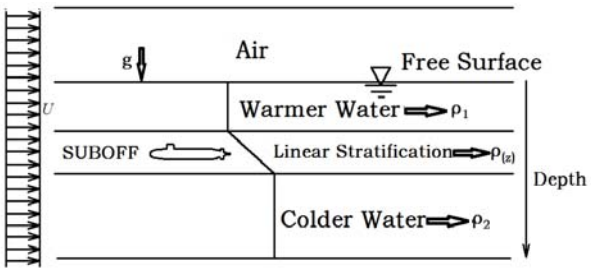

Fig.10. The stratification of the fluid

In the depth direction, the fluid of the upper layer is air, the second layer is warmer water, the middle layer is pycnocline, and the bottom layer is colder water. The thickness of each layer of water is shown in Table 3.

Tab. 3. Thickness of the different layers

	Thickness (m)
Air layer	20
Warmer water layer	20
Pycnocline layer	10
Colder water layer	40

The free surface between the air and water is located at z=25m. The vertical 3D geometry of the computational domain is shown in Figure 11.

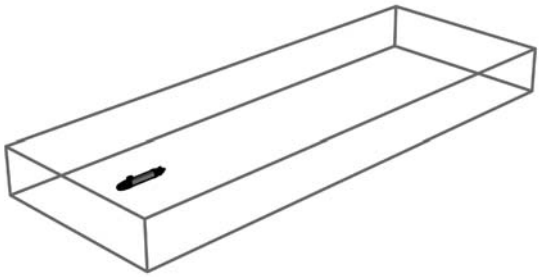

Fig.11. Calculation domain diagram of the Suboff

Tab. 4. Different cases of the simulations

Cases	Speed(kn)	Depth(m)	Density gradient(kg·m^{-4})
1	10	25	0.5
2	20	25	0.5
3	30	25	0.5
4	20	15	0.5
5	20	35	0.5
6	20	25	0.1
7	20	25	1.0

In the simulations, the depths of the submarine are 15m, 25m and 35m respectively. This can be satisfied that the submarine positions are located in the upper, middle and lower of the pycnocline layer. So that the influence of the position of the pycnocline layer relative to the submarine on the wake field can be studied. Therefore, the combinations of the speed, submarine depth and density gradient are shown in Table 4. The comparative analysis of working conditions 1, 2 and 3 can be used to study the influence of submarine speed on the internal wave and free surface wave field. The comparison of working conditions 2, 4 and 5 can be used to analyze the influence of submarine depth on the wave field. The comparative analysis of working conditions 2, 6, and 7 can study the influence of ocean environmental parameters, i.e., the strength of the pycnocline layer on the wake field.

The basic principle when meshing the computational domain is to meet the requirements of the wall y+ of the submarine. Then the grid is gradually transiting outwards. There are also separately refined at the appendage of the submarine. The free surface is refined with a custom anisotropic cutting body mesh to ensure at least 10 grids in the wave height direction. The wavelength can be estimated by the surface ship wave-making empirical formula in wave

analysis theory. It shows that when the speed of the submarine is 10, 20 and 30 knots, the wavelength is about 16.95m, 67.79m and 152.53m separately. The computational domain size is enough to capture several wave patterns. In addition, simple refines is performed near the pycnocline layer which has a height of 10 m in order to capture the internal wave field. The final grid number is about 10 million. Figure 11 is the schematic diagram of the meshes in the bow and stern of the Suboff submarine.

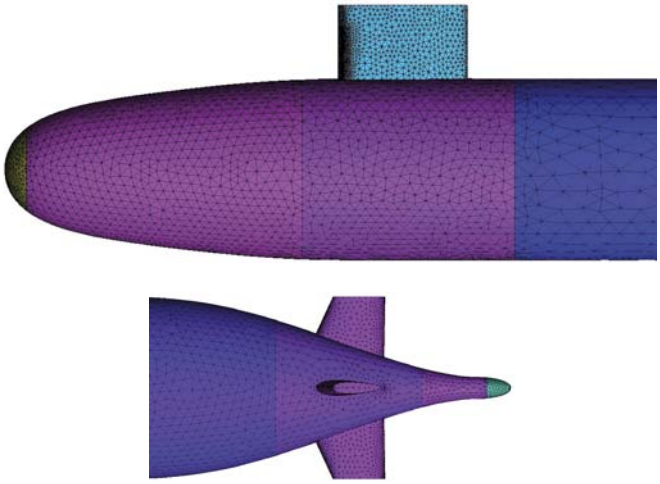

Fig. 12. Meshes around the bow and stern of the Suboff

INFLUENCE OF THE SUBMARINE SPEED ON THE FREE SURFACE

Simulations are conducted for the conditions 1, 2, and 3 in Table 4. The submarine depth is 25m, the density gradient is about 0.5kg•m^{-4}, and the speeds of the submarine are 10kn, 20kn and 30kn respectively. The simulation results are compared with each other and the influence of the submarine speed on the free surface waves is analyzed. The free surface wave pattern at different speed is shown in the Figures 13.

In summary, when the submarine sails in the stratified flow, obviously waves are generated on the free surface. The shape of these waves is similar to the Kelvin wave of a ship. As the speed of the ship increases, the wavelength of the surface wave increases gradually, which can reach to 118.49m at a speed of 30kn. At the same time, the wave height is gradually increased. The height of the waves at the speed of 10kn is on the order of centimeters. At the speed of 20kn, the wave height can be the order of decimeter. When the speed is 30kn, the maximum height of the surface wave is 1.3m. The Kelvin angle gradually decreases with the increase of the speed. When the speed is 10kn, the lateral propagation range of the scattered wave reaches 350m. When the speed is 30kn, the longitudinal propagation range of the transverse wave reaches 473.97m. At the same time, the pycnocline at the stern of the Suboff will form a catastrophic region, the thickness becomes smaller, and the length is equivalent to the length of the submarine. As the speed increases, the catastrophic region will form faster and faster. When the speed is 10kn, it uses 20 seconds to form a complete mutation area. But at the speed of 20kn and 30kn, the time to form complete catastrophic region can be reduced to 10s and 5s respectively. As the speed of the Suboff increases, the divergence intensity of the free surface flow field also gradually increases, showing a similar shape to the surface wave, and the roughness changes of the free surface are different.

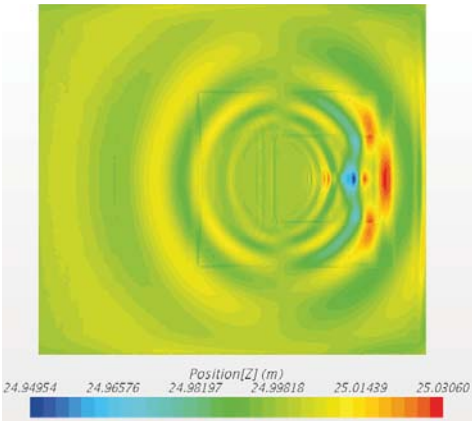

(a) Density gradient =0.5kg·m^{-4},v=10kn,t=40s

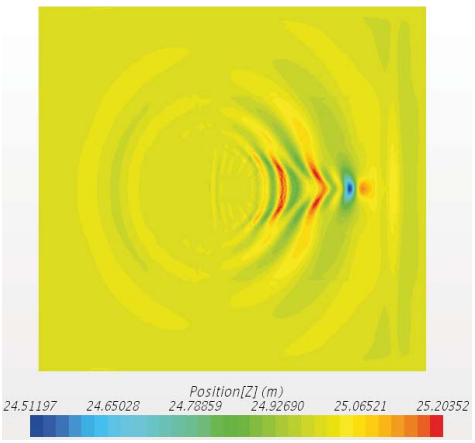

(b) Density gradient =0.5kg·m^{-4},v=20kn,t=40s

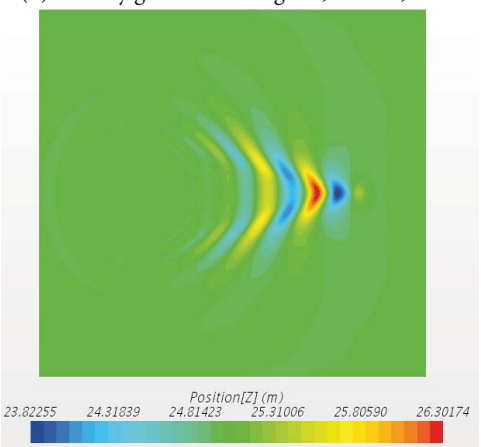

(c) Density gradient =0.5kg·m^{-4},v=30kn,t=40s

Fig.13. Wave pattern of the free surface at different speed

INFLUENCE OF THE SUBMARINE DEPTH ON THE FREE SURFACE WAVES

In the cases of 2, 4 and 5 in Table 4, the speed of the Suboff submarine are all 20kn, the gradient density of the pycnocline is 0.5kg•m^{-4}, and the depths of submarine are 25m 15m, and 35m respectively. As a result, the impact of the submarine depth on the wake field is studied.

Fig. 14a is a wave pattern diagram of the free surface wave-making with a depth of 15m and the time t=40s. At that time, about 5 complete waveforms are formed on the free surface. The longitudinal propagation distance reaches to 323.1m, and the lateral propagation distance reaches to 152.3m. In the case of 35m depth, there are about three complete waveforms on the free surface at t=40s, but compared to the depth of 25m and the depth of 15m, since the submarine is located below the pycnocline, the free surface waveform is greatly affected by the internal wave. The wave pattern is domain by the scattered waves. The Kelvin angle is relatively large. The longitudinal propagation distance is about 276.8m, and the lateral propagation distance is about 370.6m. In summary, as the submarine depth increases, the wave height of the free surface wave is gradually reduced. When the depth is 15m, the maximum crest is 1.02m. When the submarine depth is increases to 25m, the maximum crest is 0.36m. When the depth of the submarine continues to increase to 35m, the maximum crest is reduced to 0.15m. At the same time, when the submarine is below the pycnocline, the free surface wave pattern is greatly affected by the internal wave, which is mainly the scattered wave. The propagation distance is large. In the scale which is equivalent to the length of the submarine, the pycnocline becomes thicker behind the submarine and forms a bulge downward. When the submarine is above the pycnocline, the free surface wave pattern is mainly determined by the surface wave mode. The Kelvin angle is relatively smaller. The longitudinal propagation distance is larger and the pycnocline behind the submarine will formed a uplift.

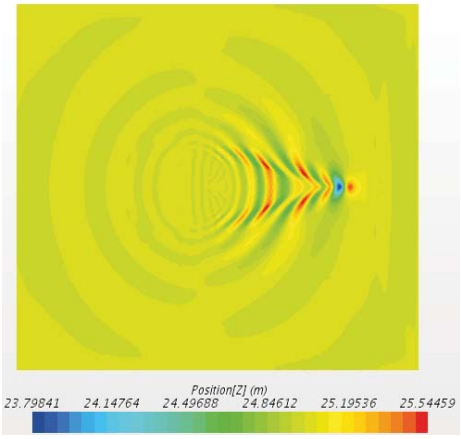

(a) Density gradient =0.5kg·m^{-4},h=15m,t=40s

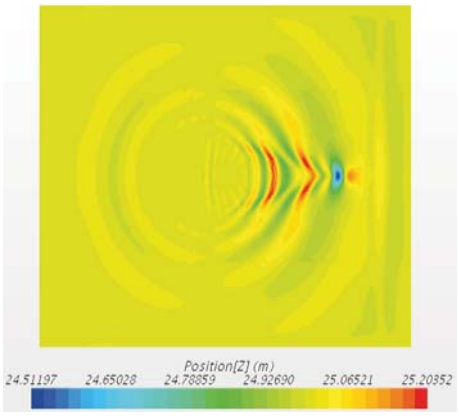

(b) Density gradient =0.5kg·m^{-4},h=25kn,t=40s

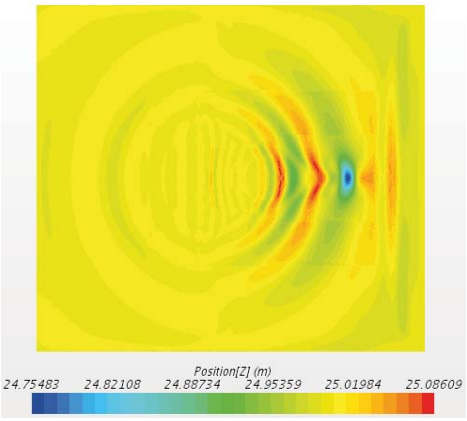

(b) Density gradient =0.5kg·m^{-4},h=35m,t=40s

Fig. 14. Wave pattern of the free surface at different submarine depth

INFLUENCE OF THE GRADIENT DENSITY GRADIENT ON THE FREE SURFACE WAVE FIELD

Comparison between the cases of 6, 2 and 7 in Table 4 can examine the effect of different density gradients on surface wave pattern. The speed of the submarine is 20kn, the submarine depth is 25m, and the gradient density gradient are 0.1 kg•m^{-4} ,0.5 kg•m^{-4}and 1.0 kg•m^{-4} respectively.

Fig. 15(a) is a diagram showing the free surface wave pattern at t = 40 s in the case of a density gradient of 0.1 kg•m^{-4}. The figure shows that there are about four complete wave patterns appearing on the free surface. The longitudinal propagation distance is 307m, and the lateral propagation is about 257.6m. The distance between the second crest and the third crest is far. Fig. 15(c) is a wave pattern of the free surface at t = 40 s in the case of a density gradient of 1.0 kg•m^{-4}. When the time t=40s, about four wave patterns appear on the free surface. The longitudinal propagation distance is about 298m, and the lateral propagation distance is about 261.3m. In summary, the change of the density gradient of the pycnocline has little effect on the free surface wave pattern and the dispersion intensity of the free surface. When the speed and the depth of the submarine are constant, the wave height and wavelength of the surface wave and the Kelvin angle

remain unchanged. Yet the effect of the change in density gradient is weak.

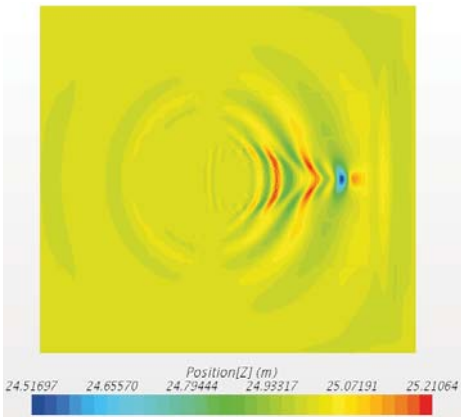

(a) Density gradient =0.1kg·m^{-4},v=20kn,t=40s

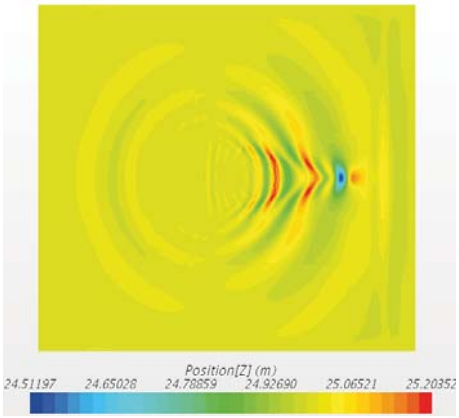

(b) Density gradient =0.5kg·m^{-4},v=20kn,t=40s

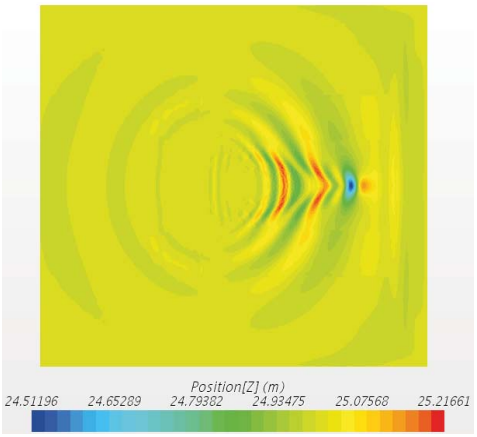

(c) Density gradient =1.0kg·m^{-4},v=20kn,t=40s

Fig.15. Wave pattern of the free surface at different pycnocline

CONCLUSIONS

This study has presented a methodology for the numerical simulation of the stratified flows. Then, using the established numerical simulation method, the stratified flows around a cylinder and the real-scale Suboff submarine are analyzed. The problem of free surface wave-making of the Suboff submarine moving in a stratified flow is investigated. The effects of speed, submarine depth and density gradient on the free surface wave are investigated.

1. At the condition of Fr=0.018 and Re=12, the wake streamlines of the numerical results for the cylinder are qualitatively consistent with the experimental results. The velocity profile of the upstream and the downstream with the time are the same between the numerical results and experimental results. The peaks and troughs of the velocity are similar for the tow results and the error ratio is less than 2%.

2. When it comes to the turbulent model, it is most reasonable to simulate the stratified flow by using the RSM model which is not restricted by the isotropy assumption. The use of $k-\omega$ based DES model to simulate the flow around the cylinder and under the condition of high Fr number can get results of good agreements with the experiments. This fully shows that the proposed model for stratified flow based on the DES model can well simulate the stratified wake at high Fr number.

3. When the Suboff submarine is proceeding in the density mixed stratified flow, the Kelvin ship wave is formed on the free surface. The crests and troughs gradually propagate to the far fields from the corresponding position above the submarine. Both transverse wave and scattered wave exist. The divergence intensity distribution of the free surface exhibits a shape similar to the wave pattern. The roughness at different positions is different. At the same time, due to the disturbance of the submarine, the thickness of the pycnocline near the submarine tail will change to a certain extent, forming a catastrophic area or a raised area corresponding to the length of the submarine. These changes can be propagated to the far wake field.

4. With the increase of the speed of the submarine, the wavelength and wave height of the free surface wave are gradually increasing. The Kelvin angle gradually decreases. With the increase of the submarine's depth, the wave height of the free surface wave is gradually reduced, and the waves pattern also change greatly. Relative to the speed and submarine depth, the change of the gradient density gradient has little effect on the free surface wave field. The wavelength, wave height and shape of the Kelvin wave on the free surface remain basically the same, and the amplitude of the divergence intensity of the flow field is nearly the same. The variation characteristics of the pycnocline at the submarine tail are mainly determined by the relative positions of the submarine and the layer, which are also less affected by the density gradient.

ACKNOWLEDGEMENTS

This paper is supported by National Natural Science Foundation of China (No. 51779053).

REFERENCES

1. Wang, J., You, Y.X., Hu, T.Q.: The Characteristics of Internal Waves Generated by a Revolution Body in a Stratified Fluid

with a Pycnocline. *Acta Physica Sinica,* 2012, 61(7), Pp. 074-701.

2. Ouchi, K.: Recent Trend and Advance of Synthetic Aperture Radar with Selected Topics. *Remote Sensing,* 2013, 5(2), Pp.716-807.

3. Spedding, G.R.: Wake Signature Detection. *Annual Review of Fluid Mechanics,* 2014, 46, Pp. 273-302.

4. Miles, J.W.H.: Lee Waves in a Stratified Flow. Part 2. Semi-Circular Obstacle. *Journal of Fluid Mechanics*, 1968, 33(4), Pp. 803-814.

5. Long, R.R.: Some Aspects of the Flow of Stratified Fluids. *Tellus*, 1955, 7(3), Pp. 341-357.

6. Lighthill, M.J.: *Hyperbolic Equations and Waves, Springer, New York*, 1970.

7. Stevenson, T.N.: Some Two-Dimensional Internal Waves in a Stratified Fluid. *Journal of Fluid Mechanics,* 1968, 33(4), Pp.715-720.

8. Stevenson, T.N., Chang, W.L., Laws, P.: Viscous effects in lee waves. Geophysical and Astrophysical Fluid Dynamics, 1979, 13(1), Pp. 41-151.

9. Boyer, D.L., Davies, P.A., Fernando, H.: Linearly Stratified Flow Past a Horizontal Circular Cylinder. *Philosophical Transactions of the Royal Society of London A: Mathematical, Physical and Engineering Sciences*, 1989, 328(1601), Pp. 501-528.

10. Xu, Y., Fernando, H.J., Boyer, D.L.: Turbulent Wakes of Stratified Flow Past a Cylinder. *Physics of Fluids,* 1995, 7(9), Pp. 2243-2255.

11. Meunier, P.: Stratified Wake of a Tilted Cylinder. Part 1. Suppression of a Von Kármán Vortex Street. *Journal of Fluid Mechanics*, 2012, 699, Pp.174-197.

12. Bosco, M., Meunier, P.: Three-dimensional instabilities of a stratified cylinder wake. *Journal of Fluid Mechanics*, 2014, 759, Pp.149-180.

13. Winters, K.B., Armi, L.: Hydraulic control of continuously stratified flow over an obstacle. *Journal of Fluid Mechanics*, 2012, 700, Pp. 502–513.

14. Esmaeilpour, M., Martin, J.E., Carrica, P.M.: Near-Field Flow of Submarines and Ships Advancing in a Stable Stratified Fluid. *Ocean Engineering*, 2016, 123, Pp.75–95.

15. Yu, C., Feng, Z., Jun, Z.: Numerical Simulation of Internal Waves Excited by a Submarine Moving in the Two-Layer Stratified Fluid. *Journal of Hydrodynamics, Ser. B,* 2006, 18(3), Pp. 330-336.

16. Frank, J.M., Alain, P.: International one-atmosphere equation of state of seawater. *Deep Sea Research*, 1981, 28(6), Pp. 625-629.

17. Yaacof, N.A., Qamaruzzaman, N., Yusup, Y.: Comparison method of odour impact evaluation using calpuff dispersion modelling and on-site odour monitoring. *Engineering Heritage Journal*, 2017, 1(1), Pp. 01-05.

18. Yue, X.G., Ashraf, M.A.: Analysis of The Function Relations Between the Depth Of Gap Or Slot And The Speed Of Vibra tion In Millisecond Multiple-Row Holes Blasting. *Engineering Heritage Journal*, 2018, 2(1), Pp. 01-04.

19. Tian, X.C., Li, Q.H., He, C.S., Cai, Y.G., Zhang, Y., Yang, Z.G.: Design and experiment of reciprocating double Track Straight Line Conveyor. *Acta Mechanica Malaysia*, 2018, 2(2), Pp. 01-04.

20. Yan, Z.H.: Modeling and Kinematics Simulation Of Plane Ten-Bar Mechanism Of Warp Knitting Machine Based On Simcape/Multibody. *Acta Mechanica Malaysia*, 2018, 2(2), Pp. 15-18.

21. Yu, Z.C.: An Improved Infrared and Visible Image Fusion Algorithm Based on Curvelet Transform. *Acta Electronica Malaysia*, 2017, 1(1), Pp. 12-14.

22. Zamanian, P., Kasiri, M.: Investigation of Stage Photography In Jee Lee's Works And Comparing them With The Works Of Sandy Skoglund. *Acta Electronica Malaysia*, 2018, 2(1), Pp. 01-06.

CONTACT WITH THE AUTHORS

Kaiye Hu, Ph.D.
email: hukaiye@126.com

College of Shipbuilding Engineering
Harbin Engineering University
Harbin Heilongjiang
150001
China